Threshold Voltage Control in $Al_{0.72}Ga_{0.28}N$/AlN/GaN HEMTs by Work-Function Engineering

Guowang Li, *Student Member, IEEE*, Tom Zimmermann, *Member, IEEE*, Yu Cao, Chuanxin Lian, *Member, IEEE*, Xiu Xing, *Student Member, IEEE*, Ronghua Wang, Patrick Fay, *Senior Member, IEEE*, Huili Grace Xing, *Member, IEEE*, and Debdeep Jena, *Member, IEEE*

***Abstract*—The first demonstration of high-Al-composition ($> 70\%$) AlGaN high electron mobility transistors (HEMTs) is reported. High electron mobility ($\sim$1300 cm^2/Vs at room temperature) was achieved in novel high-Al-composition AlGaN 2-D electron gas structures. The threshold voltages (V_{th}) of $Al_{0.72}Ga_{0.28}N$/AlN/GaN HEMTs were shifted from -1.0 to -0.13 V by employing different gate metal stacks, Al/Au and Ni/Au, respectively. With a 4-nm Al_2O_3 gate dielectric on top of the nitride heterostructures, the $\sim$0.9-eV work-function difference between Al and Ni induced $\sim$0.9-V V_{th} shift in the pairs of the Al/Au and Ni/Au gate HEMTs, which indicates that the Fermi level is unpinned at the ALD Al_2O_3/AlGaN interface. The results were reproducible for HEMTs of various gate lengths. The results suggest that it is possible to obtain enhancement- and depletion-mode AlGaN HEMTs using work-function engineering which can enable integrated monolithic digital circuits without postgrowth recess etching or ion implantation.**

***Index Terms*—Enhancement (E) mode, gallium nitride, molecular beam epitaxy (MBE), threshold voltage (V_{th}), transistor, work function.**

I. Introduction

Low-Al-composition ($< 40\%$) AlGaN/GaN-based HEMTs have proven to be a promising technology platform for high-power and high-frequency applications [1] since the first demonstration of depletion-mode (D-mode) devices in 1993 [2]. Enhancement-mode (E-mode) AlGaN HEMTs are desired for digital applications and low-loss high-power switching. Several techniques have been developed to control the threshold voltage (V_{th}) for achieving E-mode HEMTs. For example, gate-recess process [3], fluoride-based [4] and oxygen [5] plasma treatment, p-AlGaN gate with conductivity modulation [6], and nonpolar a-plane [7] and m-plane [8] HEMTs have been investigated. Unlike many other III-V semiconductors such as AlGaAs [9], the surface Fermi level is weakly pinned for AlGaN. Schottky barrier heights were observed to vary with different work-function (ϕ_m) metals [10], indicating a distinct possibility of using different gate metal stacks to adjust the threshold voltage. The E-mode AlGaN HEMTs with annealed Pt-based gate metal stacks have been demonstrated [11]. However, all gate-metal-stack-related threshold-voltage-control studies have been performed on low-Al-composition ($< 40\%$) AlGaN, which restricts vertical scaling for high-speed operation. On the other hand, compared to AlN/GaN HEMTs [12], Al-rich AlGaN can potentially facilitate low ohmic contact resistance due to a smaller band gap than AlN. Due to the higher 2-D electron gas (2DEG) density and lower sheet resistance at the same AlGaN barrier thickness, a high-Al-composition AlGaN layer is preferable to boost the power and RF performance of deep submicrometer HEMTs. In this letter, we report the first high-Al-composition ($> 70\%$) AlGaN barrier HEMTs and demonstrate that the threshold voltages can be modified by gate work-function engineering. This finding enables V_{th} engineering without the need for either ion implantation or precise recess etching, and therefore is well suited for scaling.

Manuscript received April 27, 2010; revised May 31, 2010; accepted June 7, 2010. Date of publication July 12, 2010; date of current version August 25, 2010. This work was supported in part by the Air Force Office of Scientific Research (Dr. Kitt Reinhardt), by the Office of Naval Research (Dr. Paul Maki), and by the Defense Advanced Research Projects Agency (Dr. John Albrecht, HR0011-10-C-0015). The review of this letter was arranged by Editor G. Meneghesso.

The authors are with the Department of Electrical Engineering, University of Notre Dame, Notre Dame, IN 46556 USA (e-mail: djena@nd.edu).

Color versions of one or more of the figures in this letter are available online at http://ieeexplore.ieee.org.

Digital Object Identifier 10.1109/LED.2010.2052912

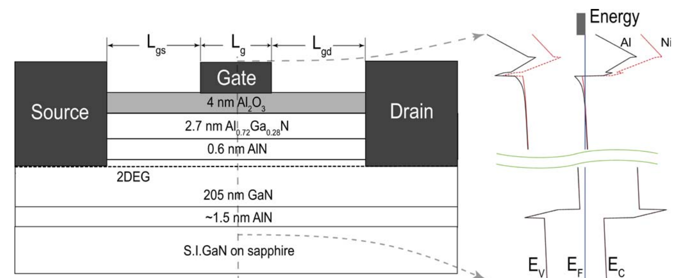

Fig. 1. Illustrative $Al_{0.72}Ga_{0.28}N$/AlN/GaN HEMT structures and schematic of energy band diagrams with different work-function gate metal stacks. (Solid lines) Al/Au and (dashed lines) Ni/Au.

II. Experiments

$Al_{0.72}Ga_{0.28}N$/AlN/GaN heterostructures were grown on semi-insulating GaN templates on sapphire by molecular beam epitaxy in a Veeco Gen930 system. Based on the growth conditions and high-resolution X-ray diffraction measurement, the layer structures and the Al composition of the barrier were obtained. As shown in Fig. 1, an $\sim$1.5-nm-thick AlN nucleation layer was first grown under nitrogen-rich conditions to remove buffer leakage using a polarization-dipole-induced back barrier [13], followed by a 205-nm-thick unintentionally doped GaN buffer and capped with an $\sim$0.6-nm-thick AlN spacer and an $\sim$2.7-nm-thick $Al_{0.72}Ga_{0.28}N$ as a barrier layer. The room temperature (RT) Hall-effect measurement yielded a 2DEG density of $\sim 1.6 \times 10^{13}/cm^2$ and a mobility of

0741-3106/$26.00 © 2010 IEEE

1270 cm^2/Vs, producing a sheet resistance R_{sh} of ~304 $\Omega/\square$. A 4-nm aluminum oxide gate dielectric was deposited using atomic layer deposition (ALD). After the ALD, from the RT Hall-effect measurement, R_{sh} was ~270 $\Omega/\square$ with a mobility of ~1400 cm^2/Vs and a 2DEG density of $\sim 1.6 \times 10^{13}/cm^2$. Mesas for device isolation were then formed by using BCl_3/Cl_2-based reactive ion etching. Ti/Al/Ni/Au metal stacks were deposited by using electron-beam evaporation, and spike annealed at 485 °C to obtain ohmic contacts. Transmission line method measurement on 100-μm-wide pads resulted in a contact resistance R_C of ~2.4 $\Omega \cdot$ mm and a sheet resistance of ~348 $\Omega/\square$. The high contact resistance arises from the unoptimized ohmic metal stacks and annealing conditions on the novel high-Al-composition AlGaN material. Five-hundred-nm-long gates were defined by electron-beam lithography. Al/Au (50/50 nm) and Ni/Au (50/50 nm) gate metal stacks were deposited on adjacent devices using electron-beam evaporation on the same sample. The device dimensions, as measured using a scanning electron microscope (SEM), for Al/Au and Ni/Au are as follows: $W_g/L_g =$ 50/0.49 and 50/0.51 μm and $L_{gs}/L_{sd} = 0.74/2.3$ and 0.55/2.2 μm, respectively. An illustrative HEMT structure containing the $Al_{0.72}Ga_{0.28}N$ (barrier)/AlN (spacer)/GaN (buffer)/AlN (nucleation) and the corresponding schematic energy band diagrams with Al/Au and Ni/Au gate metal stacks are shown in Fig. 1. Considering the ~0.9-eV work-function difference between Al ($\phi_m = 4.3$ eV) and Ni ($\phi_m = 5.2$ eV) [14], a larger surface Schottky barrier height results in a lower 2DEG density in the channel under the gate, shifting the threshold voltage in the positive direction.

III. Results and Discussion

The dc I–V characteristics of the HEMTs were measured by using an Agilent 4155C semiconductor parameter analyzer. As shown in Fig. 2(a), the saturated drain currents at $V_{GS} =$ +1.5 V were ~450 and ~300 mA/mm for the Al/Au and Ni/Au gate HEMTs, respectively. With the drain currents still at least two orders of magnitude higher than the gate currents, the current drive reaches ~0.5 A/mm for both the Al/Au and Ni/Au gate HEMTs at $V_{GS} = +4.5$ V and $V_{DS} = +5$ V. With lower contact resistances, higher current drives can be expected. The measured drain and gate currents of the Al/Au and Ni/Au gate HEMTs are shown in the transfer-characteristic plot in Fig. 2(b). Taking advantage of the low gate leakage combined with an insulating buffer enabled by the polarization-dipole-induced back barrier, both the Al/Au and Ni/Au gate HEMTs showed drain current on/off ratios higher than $\sim 10^5$. The low subthreshold slopes of 110 and 94 mV/dec for Al/Au and Ni/Au gate HEMTs respectively, although limited by the gate leakage, indicate a low defect interface between the ALD gate dielectric and the nitride heterostructure. From the figure, it is clearly evident that the use of the Al/Au or Ni/Au gate metal stacks shifts the I_D–V_{GS} transfer curves while maintaining a high device performance. Ni deposition at a higher temperature than Al might be responsible for device degradation in the form of a higher on-resistance [see Fig. 2(a)] and a larger gate current at $V_{GS} > +0.8$ V [see Fig. 2(b)] for the Ni-gate HEMT device.

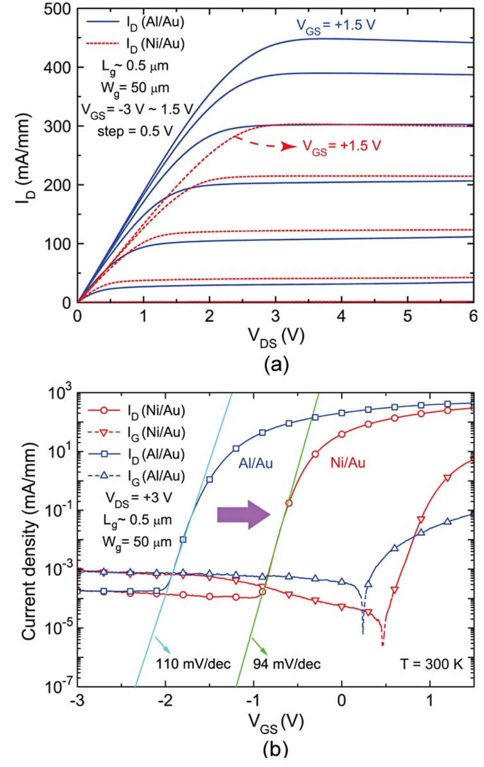

Fig. 2. (a) DC I–V characteristics of Al/Au and Ni/Au gate $Al_{0.72}Ga_{0.28}N$/AlN/GaN HEMTs. (b) Transfer characteristics of gate and drain currents of HEMTs with Al/Au and Ni/Au gate stacks.

The dc transfer characteristics of the Al/Au and Ni/Au gate HEMTs are shown in Fig. 3(a). The drain was biased at +3 V, and the devices pinched off completely at $V_{GS} = -1.52$ and -0.5 V with the criteria of $I_D^{OFF} \leq 1$ mA/mm for the Al/Au and Ni/Au gate HEMTs, respectively. The peak values of extrinsic transconductance g_m^{ext} are ~200 and ~190 mS/mm at $V_{GS} = 0.03$ and 0.8 V for the Al/Au and Ni/Au gate HEMTs, respectively. The source access resistance is $R_s = R_C + R_{sh} \cdot L_{gs}$; the intrinsic transconductance g_m^{int} calculated using $g_m^{int} = g_m^{ext}/(1 - g_m^{ext} \cdot R_s)$ yields $g_m^{int} \sim 420$ and ~370 mS/mm for the Al/Au and Ni/Au gate HEMTs, respectively. This is a conservative estimation of g_m^{int} since, at the peak g_m, the actual R_s is higher under the bias. Defining the threshold voltage as the gate-bias intercept of the linear extrapolation of the drain current from the point of the peak transconductance, V_{th} of -1.0 and -0.13 V were extracted for the Al/Au and Ni/Au gate HEMTs, respectively. The ~0.9-V threshold-voltage difference agrees well with the ~0.9-eV work-function difference of Al and Ni. In pairs of various gate lengths of the Al/Au and Ni/Au gate HEMTs, a similar threshold-voltage shift (~0.9 V) was also observed. Based on metal-induced gap states and charge neutrality level theories [15] in the wide-band-gap high-Al-composition AlGaN, the change of V_{th} (~0.9 V) equals to the difference of the gate metal work function (~0.9 V), indicating that the ALD Al_2O_3/AlGaN interface Fermi level is unpinned. For 1-μm-long Ni/Au gate HEMTs, the drain-induced-barrier-lowering factor was extracted to be ~20 mV/V showing a long channel characteristic. The temperature dependence of family I–V curves was measured on a 2-μm-long Ni/Au gate HEMT, and the knee voltages did not change appreciably with varying

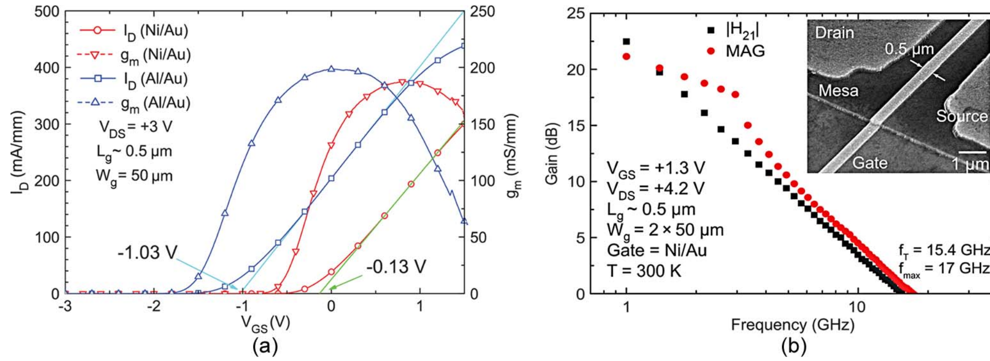

Fig. 3. (a) DC transfer characteristics show ∼0.9-V threshold-voltage shift between Al/Au and Ni/Au gate HEMTs. (b) RF performance of the 500-nm-gate-length Ni/Au gate HEMT exhibits $f_T = 15.4$ GHz and $f_{\max} = 17$ GHz. Inset shows a finished device.

temperature $(80\ \mathrm{K} \leq \mathrm{T} \leq 400\ \mathrm{K})$, indicating that the device performance is limited by the high contact resistance. The device 3-terminal breakdown was measured on a 3-μm-long Ni/Au gate HEMT with $L_{\mathrm{gs}}/L_{\mathrm{sd}} = 1\ \mu\mathrm{m}/5\ \mu\mathrm{m}$ and $V_{\mathrm{GS}} = 0$ V, and $I_{\mathrm{D}}/I_{\mathrm{G}}$ reached 10/2.1 μA/mm at $V_{\mathrm{DS}} = +100$ V, indicating respectable breakdown characteristics.

High-frequency measurements were performed using an Agilent 8722D network analyzer. The current-gain and power-gain cutoff frequencies $(f_T, f_{\max})$ were measured to be 15.4 and 17 GHz, respectively, for a $0.5 \times 100\ \mu\mathrm{m}^2$ Ni/Au gate HEMT. The HEMT was biased at $V_{\mathrm{GS}} = +1.3$ V and $V_{\mathrm{DS}} = +4.2$ V. Fig. 3(b) shows the short-circuit current gain $(|H_{21}|)$ and the maximum available gain as a function of the frequency of the Ni/Au gate device, with a SEM image of the finished device shown in the inset. Although the $f_T/f_{\max}$ values are limited by the high contact resistance, the high-Al-composition AlGaN HEMTs show a potential for integrated E- and D-mode RF applications with the improvement of the ohmic contact and the scaling down of the gate lengths.

IV. Conclusion

In summary, high-Al-composition $Al_{0.72}Ga_{0.28}N$/AlN/GaN HEMTs with an ALD Al_2O_3 dielectric are reported for the first time. The threshold voltages of the HEMTs were observed to shift with different gate metals commensurate with their difference in work functions. This observation implies an unpinned Fermi level at the ALD $Al_2O_3/Al_{0.72}Ga_{0.28}N$ interface possibly due to a fixed number of interface states spread over a wide band-gap-energy window. If the contact resistances can be lowered, a better device performance is expected. High-work-function Pt $(\phi_m = 5.7\ \mathrm{eV})$ gates can enable complete E-mode operation, while a low-work-function Ti $(\phi_m = 4.3\ \mathrm{eV})$ can possibly serve as a gate metal for D-mode operation. A high-Al-composition $Al_{0.72}Ga_{0.28}N$ barrier may possibly offer a lower gate tunneling current due to a higher band gap $(E_{\mathrm{g}} \sim 5.4\ \mathrm{eV})$ and conduction band offset $(\Delta E_C \sim 1.3\ \mathrm{eV})$ with respect to GaN, compared to an AlInN barrier [16] lattice-matched to GaN $(E_{\mathrm{g}} \sim 4.4\ \mathrm{eV}, \Delta E_C \sim 0.6\ \mathrm{eV})$. The demonstration of threshold voltage shifts with work-function engineering presents an alternative method to integrate E- and D-mode devices without gate-recess etching or implantation and is well suited for the lateral and vertical scaling of nitride HEMTs for high-frequency operation.

References

[1] U. K. Mishra, P. Parikh, and Y. F. Wu, "AlGaN/GaN HEMTs—An overview of device operation and applications," *Proc. IEEE*, vol. 90, no. 6, pp. 1022–1031, Jun. 2002.

[2] M. A. Khan, A. Bhattarai, J. N. Kuznia, and D. T. Olson, "High electron mobility transistors based on a GaN/AlGaN heterojunction," *Appl. Phys. Lett.*, vol. 63, no. 9, pp. 1214–1215, Aug. 1993.

[3] C. H. Chen, S. Keller, E. Haberer, L. Zhang, S. P. DenBaars, E. L. Hu, and U. K. Mishra, " Cl_2 reactive ion etching for gate recessing of AlGaN/GaN field-effect transistors," *J. Vac. Sci. Technol. B, Microelectron. Process. Phenom.*, vol. 17, no. 6, pp. 2755–2758, Nov. 1999.

[4] Y. Cai, Y. G. Zhou, K. J. Chen, and K. M. Lau, "High-performance enhancement-mode AlGaN/GaN HEMTs using fluoride-based plasma treatment," *IEEE Electron Device Lett.*, vol. 26, no. 7, pp. 435–437, Jul. 2005.

[5] C. Y. Chang, S. J. Pearton, C. F. Lo, F. Ren, I. I. Kravchenko, A. M. Dabiran, A. M. Wowchak, B. Cui, and P. P. Chow, "Development of enhancement mode AlN/GaN high electron mobility transistors," *Appl. Phys. Lett.*, vol. 94, no. 26, p. 263 505, Jun. 2009.

[6] Y. Uemoto, M. Hikita, H. Ueno, H. Matsuo, H. Ishida, M. Yanagihara, T. Ueda, T. Tanaka, and D. Ueda, "Gate Injection Transistor (GIT)—A normally-off AlGaN/GaN power transistor using conductivity modulation," *IEEE Trans. Electron Devices*, vol. 54, no. 12, pp. 3393–3399, Dec. 2007.

[7] M. Kuroda, T. Ueda, and T. Tanaka, "Nonpolar AlGaN/GaN metal-insulator-semiconductor heterojunction field-effect transistors with a normally off operation," *IEEE Trans. Electron Devices*, vol. 57, no. 2, pp. 368–372, Feb. 2010.

[8] T. Fujiwara, S. Rajan, S. Keller, M. Higashiwaki, J. S. Speck, S. P. DenBaars, and U. K. Mishra, "Enhancement-mode m-plane AlGaN/GaN heterojunction field-effect transistors," *Appl. Phys. Express*, vol. 2, no. 1, p. 011001, Jan. 2009.

[9] H. Shen, M. Dutta, L. Fotiadis, P. G. Newman, R. P. Moerkirk, W. H. Chang, and R. N. Sacks, "Photoreflectance study of surface Fermi level in GaAs and GaAlAs," *Appl. Phys. Lett.*, vol. 57, no. 20, pp. 2118–2120, Nov. 1990.

[10] Z. Lin, W. Lu, J. Lee, D. Liu, J. S. Flynn, and G. R. Brandes, "Barrier heights of Schottky contacts on strained AlGaN/GaN heterostructures: Determination and effect of metal work functions," *Appl. Phys. Lett.*, vol. 82, no. 24, pp. 4364–4366, Jun. 2003.

[11] A. Endoh, Y. Yamashita, K. Ikeda, M. Higashiwaki, K. Hikosaka, T. Matsui, S. Hiyamizu, and T. Mimura, "Non-recessed-gate enhancement-mode AlGaN/GaN high electron mobility transistors with high RF performance," *Jpn. J. Appl. Phys.*, vol. 43, no. 4B, pp. 2255–2258, Apr. 2004.

[12] T. Zimmermann, D. Deen, Y. Cao, D. Jena, and H. Xing, "Formation of ohmic contacts to ultra-thin channel AlN/GaN HEMTs," *Phys. Stat. Sol. (C)*, vol. 5, no. 6, pp. 2030–2032, Apr. 2008.

[13] Y. Cao, T. Zimmermann, H. Xing, and D. Jena, "Polarization-engineered removal of buffer leakage for GaN transistors," *Appl. Phys. Lett.*, vol. 96, no. 4, p. 042 102, Jan. 2010.

[14] A. C. Schmitz, A. T. Ping, M. A. Khan, Q. Chen, J. W. Yang, and I. Adesida, "Metal contacts to n-type GaN," *J. Electron. Mater.*, vol. 27, no. 4, pp. 255–260, Dec. 1998.

[15] J. Robertson and B. Falabretti, "Band offsets of high Ê gate oxides on III-V semiconductors," *J. Appl. Phys.*, vol. 100, no. 1, p. 014 111, Jul. 2006.

[16] J. W. Chung, O. I. Saadat, J. M. Tirado, X. Gao, S. Guo, and T. Palacios, "Gate-recessed InAlN/GaN HEMTs on SiC substrate with Al_2O_3 passivation," *IEEE Electron Device Lett.*, vol. 30, no. 9, pp. 904–906, Sep. 2009.